Society For Biomaterials

Effect of cobalt ions on the interaction between macrophages and titanium

Mattias Pettersson [1], **Jean Pettersson** [2], **Margareta Molin Thorén** [1], **Anders Johansson** [3]

[1]Prosthetic Dentistry, Umeå University, Sweden
[2]Analytic Chemistry, BMC, Department of Chemistry, Uppsala University, Sweden
[3]Molecular Periodontology, Department of Odontology, Faculty of Medicine, Umeå University, Sweden

Received 1 September 2017; revised 12 April 2018; accepted 25 April 2018
Published online in Wiley Online Library (wileyonlinelibrary.com). DOI: 10.1002/jbm.a.36447

Abstract: Inflammation and bone reduction around dental implants are described as peri-implantitis and can be caused by an inflammatory response against bacterial products and toxins. Titanium (Ti) forms aggregates with serum proteins, which activate and cause release of the cytokine interleukin (IL-1β) from human macrophages. It was hypothesized that cobalt (Co) ions can interact in the formation of pro-inflammatory aggregates, formed by titanium. To test this hypothesis, we differentiated THP-1 cells into macrophages and exposed them to Ti ions alone or in combination with Co ions to investigate if IL-1β release and cytotoxicity were affected. We also investigated aggregate formation, cell uptake and human biopsies with inductively coupled plasma atomic emission spectroscopy and electron microscopy. Co at a concentration of 100 μM neutralized the IL-1β release from human macrophages and affected the aggregate formation. The aggregates formed by Ti could be detected in the cytosol of macrophages. In the presence of Co, the Ti-induced aggregates were located in the cytosol of the cultured macrophages, but outside the lysosomal structures. It is concluded that Co can neutralize the Ti-induced activation and release of active IL-1β from human macrophages *in vitro*. Also, serum proteins are needed for the formation of metal-protein aggregates in cell medium. Furthermore, the structures of the aggregates as well as the localisation after cellular uptake differ if Co is present in a Ti solution. Phagocytized aggregates with a similar appearance seen *in vitro* with Ti present, were also visible in a sample from human peri-implant tissue. J Biomed Mater Res Part A: 106A: 2518–2530, 2018.

Key Words: titanium, cobalt, interleukin-1β, peri-implantitis, aggregate formation

How to cite this article: Pettersson M, Pettersson J, Molin Thorén M, Johansson A. 2018. Effect of cobalt ions on the interaction between macrophages and titanium. J Biomed Mater Res Part A 2018:106A:2518–2530.

INTRODUCTION

Dental implants are used as a standard treatment of edentulism worldwide. Millions of dental implants have been installed since the discovery of osseointegration of a titanium implant in a human in the 1960s.[1] Most dental implants on the market are produced using commercial pure (c.p.) titanium (Ti), but implants with alloys of Ti are also available. As a material for dental implants, Ti is favorable because it has good material characteristics such as mechanical strength, corrosion resistance, chemical stability, and biocompatibility. Ti is considered to be relatively inert, and because of the thin TiO_2 layer formed on the surface, it is highly resistant to corrosion.[2] Corrosion experiments *in vivo* show that Ti, stainless steel and cobalt-base have a similar polarization resistance, which suggests that high corrosion resistance is not the most essential property for a material to be biocompatible.[3] Due to the high cost of gold, base alloys (for example, Co-Cr, Ni-Cr, Ti)[4] have been used as common alternatives in the framework for implant supported dentures.

During the last decade, a rising number of papers has been published about inflammatory problems and bone loss around dental implants, so-called peri-implantitis.[5–7] Studies have confirmed a wide range in the prevalence, 12.9–28%, in different study populations.[8–12] A troubling high prevalence of peri-implant mucositis,[9–12] which is assumed to be a precursor to peri-implantitis,[13] is also reported. Ongoing research is trying to understand why some patients suffer from peri-implantitis and others do not. Various theories about the cause of this inflammatory reaction around dental implants are discussed in the literature.[14–16] The main current hypothesis is that bacterial plaque on the implant leads to an immunological response in the soft and hard tissue against bacterial products and toxins, and the resulting inflammation causes loss of supporting bone.[17–19]

Albrektsson et al.,[20] disagree with that bacterial infection hypothesis, and propose that peri-implantitis is a consequence of an aggravated foreign body response against the implant.

Correspondence to: M. Pettersson; e-mail: mattias.p.pettersson@.umu.se
Contract grant sponsor: Svenska Tandläkare-Sällskapet
Contract grant sponsor: Västerbotten Läns Landsting; contract grant number: TUA, VLL 1147-2014

Aseptic loosening of orthopedic implants is described as a immunological response against wear particles eroded from the implant and was first reported by Harris et al.[21] It is well established in orthopedic research that wear debris and nanoparticles from different metals can cause osteolysis by activation and secretion of the pro-inflammatory cytokines (for example, interleukin (IL)-1β, IL-6, tumor necrosis factor (TNF)-α, and prostaglandin E2 (PGE2).[22–28]

In dentistry, very little has been discussed about this particle-induced inflammatory process that could occur around a dental implant. As in osteolysis around an orthopedic implant,[29] peri-implantitis shows a similar infiltration of macrophages, and the macrophage infiltration is more pronounced in peri-implantitis than in an infectious disease such as periodontitis.[30]

In a previous *in vitro* study, we showed that Ti ions form particles that can act as secondary stimuli, which can activate and release IL-1β from human macrophages.[31] This cytokine release from macrophages can act in synergy with an infection-induced inflammation and cause an imbalance in the host response. IL-1β is one of the most potent cytokines and initiates inflammation by a long list of effects: it promotes leukocyte migration from the blood stream into the infected tissue. It induces fever, increased expression of adhesion molecules, and induced expression of genes that encode for IL-6 and nitric oxidase synthase.[32–34]

Irshad et al. showed that peri-implant granulation tissue fibroblasts, which are exposed to TiO_2 in combination with *Porphyromonas gingivalis* or separately, can induce a pro-inflammatory response.[35] It has been suggested that Ti ions can elevate the sensitivity of gingival epithelial cells to microorganisms and cause a monocyte infiltration in the gingiva.[36] These findings have been confirmed by Wachi et al. who also found that Ti ions induced monocyte infiltration and osteoclast differentiation in the epithelium.[37] Recruited macrophages will phagocytize nanoparticles of Ti-protein aggregates into the phagolysosomes and try to degrade them.[38,39] High Ti content in the phagocytosed particles will protect them from proteolysis and result in intracellular disruption of the lysosome membrane. This will induce the assembly of the inflammasome complex, which will activate and release pro-inflammatory cytokines.[40]

Surface roughness might affect osteoclast differentiation by activation of the RANK (receptor activator of nuclear factor κB)-TRAF-6 (TNF receptor associated factor 6) signaling network.[36,41] In addition, it has been shown that Co can affect macrophage activation.[42]

The aims of this study were to investigate: (1) if the Ti-induced activation and release of IL-1β from human macrophages is affected by the presence of Co, (2) if Co ions affect Ti aggregate formation in a physiological solution, (3) if Co ions affect uptake of the Ti-protein aggregates into macrophages, and (4) if similar aggregates can be found in biopsies of human peri-implantitis tissue. The null hypothesis is that addition of Co to a Ti solution will not affect the Ti-protein aggregation or the Ti-induced release of active IL-1β from human macrophages.

MATERIALS AND METHODS

Growth medium and cell culture

A human acute monocytic leukemia cell line, THP-1 (ATCC® TIB-202™, Manassas, VA) used and cultured in Roswell Park Memorial Institute (RPMI) 1640 medium containing 10% fetal bovine serum (FBS) with a supplement of penicillin-streptomycin (Sigma-Aldrich, St. Louis, MO).[43] Phosphate buffered saline (PBS) and RMPI 1640 without FBS supplements were used as control solutions.

Stimulation agents

Plasma standard solutions, Specpure, 1000 μg/mL, for cobalt (Co), Ti and chromium (Cr), were from Alfa Aesar GmbH & Co. KG (Karlsruhe, Germany). The standards have a content of acid to stabilize the metal in an ionic form: 5% nitric acid (HNO_3) for Co; 5% HNO_3/trace (tr) hydrogen fluoride (HF) for Ti; and 5% HCl for Cr. Acidity of the ion solutions of Co, Cr, and Ti was determined with a pH meter (Beckman), adjusted to pH 7.2 with 1 M NaOH, and diluted to a concentration of 200 μM in RPMI 1640 containing 10% FBS. In the present study, the test agents were tested in combination with Ti in a concentration of 100 μM. Tested combinations were Ti-Co and Ti-Cr, in the concentration range 100 μM Ti plus 12.5, 25, 50, or 100 μM of the other ions.

Cell stimulation

One hundred microliter of THP-1 cells suspended in RPMI 1640, containing 10% FBS with a supplement of penicillin-streptomycin (Sigma-Aldrich; St Louis, MO) were put into each well of 48-well culture plates with a cell concentration of 10^6 cells/mL. THP-1 cells were differentiated into a macrophage phenotype by adding Phorbol 12-Myristate 13-Acetate (PMA) (Sigma-Aldrich) to a concentration of 5 nM/mL and incubated at 37°C under 5% CO_2 for 24 h. Then the culture medium was replaced with fresh culture medium without PMA. The fresh medium contained lipopolysaccharides (LPS) from *Escherichia coli* (Sigma-Aldrich), 100 ng/mL, and the cells was cultured for another 6 h. After 6 h of LPS priming of the cells, the culture medium was replaced with RPMI 1640 + 10% FBS containing the test agents. All cells exposed to test agents were exposed to Ti at a concentration of 100 μM, and the other agents, Co, Cr, were at 12.5, 25, 50, or 100 μM ($n = 12$/concentration). Cells exposed to 100 μM Ti were used as positive control ($n = 24$) and cells only primed with LPS and growth medium were used as negative control ($n = 24$). Cells were exposed to the tested agents for 24 h and then the experiment was terminated. Cells used for transmission electron microscopy (TEM) were only challenged with Ti at a concentration of 100 μM or in combination with 100 μM Co during the 24 h prior to the 6 h of priming by *E. coli* LPS. Data were normalized for comparison between experiments. IL- β released from cells exposed to Ti at a concentration of 100 μM was set as 100%, and cells only primed with *E. coli* LPS were used as negative control.

One milliliter of THP-1 cells was added to each well in 12-well culture plates with a cell concentration of 10^6 cells/mL and differentiated into macrophages with PMA. After

24 h of culturing at 37°C under 5% CO_2, RPMI 1640 + 10% FBS was changed and *E. coli* LPS at a concentration of 100 ng/mL was added. After 6 h of priming of the cells with *E. coli* LPS, RPMI 1640 + 10% FBS was changed, and Ti 100 μM ($n = 12$) or Co 100 μM ($n = 12$) was added. After 24 h of exposure to the test agent, the experiment was terminated. The supernatant from each culture well was transferred to 2 mL plastic tubes by pipetting, and 1 mL of 0.1% Triton X-100 was added to lyse of the cells. After 4 h, the lysed cells were transferred to 2 mL plastic tubes for analysis of the content of Ti with inductively coupled plasma atomic emission spectroscopy (ICP-AES).

Cytotoxicity

To measure the *in vitro* cytotoxicity against the stimulatory agents; in the tested concentrations ($n = 5$/concentration); positive control ($n = 12$); and negative control ($n = 12$), the neutral red uptake (NRU) assay was used, following the protocol described by Repetto.[44] Neutral red (3-amino-7-dimethylamino-2-methylphenazine hydrochloride) uptake was used as a quantitative estimation of cell viability for cells in cell culture. The cells were exposed to the neutral red dye in the culture medium for 24 h during which time the dye passes through the cell membrane and is incorporated into the lysosomes in viable cells. Then the culture medium was changed to a medium without neutral red, and an acidified ethanol solution was added to extract the dye. The culture medium was transferred by pipetting to a spectrophotometer vial and absorbance of the extracted neutral red was measured with a spectrophotometer (SPECTRAMax^{TM} 340; Molecular Devices, LLC., Sunnyvale, CA) at wavelength 540 nm, using the blanks without cells as the reference. The NRU in the control cells cultured in plain medium was considered as 100% viable cells.

Cytokine analyses with ELISA

A "sandwich" ELISA (the Human IL-1β DuoSet ELISA; R&D Systems, Minneapolis, MN) was used to detect the secretion of active IL-1β from THP-1 cells into the supernatant after 6 h of priming with *E. coli* LPS and then 24 h exposure to the test agents. Then, the supernatant was removed by pipetting, and the ELISA was performed on the supernatant following the protocol provided by the manufacturer. To quantify the amount of secreted IL-1β into the supernatant, a spectrophotometer (SPECTRAMax^{TM} 340) measuring at wavelength 450 nm was used.

Centrifugation test

To investigate protein aggregation with Ti alone or in combination with Co, Ti solution or Ti + Co solution were suspended in RPMI 1640 ± 10% FBS, each at a concentration of 100 μM. One mL of the test solutions was centrifuged at 12,000g for 10 min in a Sigma 4K15C (Sigma Laborzentrifugen GmbH, Osterode am Harz, Germany) centrifuge at 22°C. The supernatant was transferred to a new plastic tube by pipetting, and the formed pellet was resuspended in PBS or RPMI 1640. The content of Ti in the pellet ($n = 3$) and in the supernatant ($n = 3$), were analyzed with ICP-AES. Noncentrifuged test solutions were also analyzed with ICP-AES to ensure that the total concentration of Ti (100 μM) could be measured ($n = 3$).

Filtering test

This test investigated the size of the formed protein aggregates in the cell medium with Ti or with Ti + Co. Solutions of Ti ($n = 3$) and Ti + Co ($n = 3$) in RPMI 1640 + 10% FBS were passed through a 0.22-μm sterile filter (Merck Millipore, Billerica, MA). The filtered test solutions were then analyzed with ICP-AES for Ti content, and unfiltered solutions were used as control.

ICP-AES analyses

Solutions. The calibration solutions were diluted from commercial 1000 μg/mL Ti or Co stock solutions that were manufactured by Spectrascan, Norway.

MQ-water was freshly prepared by a Milli-Q gradient A10 Millipore system that gives 18.2 M-ohm resistance and <5 ppb TOC (total organic carbon).

Instrument. An Inductively Coupled Plasma-Atomic Emission Spectrometer Spectro Cirros ^{CCD}, Spectro, Kleve, Germany was used for all elemental measurements. The settings were according to the manufacturer's recommendations, and the nebulizer was a modified Lichte nebulizer with a cyclonic spray chamber. Sample uptake rate was 2 mL per minute. The emission lines used were 228.616 nm for Co and 334.941 nm for Ti.

Method. The cell test solutions were diluted 10-fold with MQ-water before analysis with ICP-AES. The sample solutions were nebulized 45 s before the test, and the analytical signals were integrated simultaneously 3 times 24 s. The average was used for further calculations. Calibrations were performed by an ordinary matrix-matched external calibration curve.

Protein analyses and cell uptake with transmission electron microscopy

The Ti standard, Specpure, 1000 μg/mL, was suspended in RPMI 1640 ± 10% FBS to a concentration of 200 μM. The Ti + Co standard solution was prepared similarly to a concentration of 200 μM Ti + 200 μM Co in RPMI 1640 + 10% FBS. 2 mL of each of these two solutions was mixed and centrifuged at 12,000g for 10 min at room temperature. The supernatant was removed by pipetting, and the pellet was re-suspended in RPMI 1640 without FBS to avoid contamination with new serum proteins. 3.5 μL of each sample was applied to glow-discharged formvar and carbon-coated nickel (Ni)-grids. The grid was washed and negatively stained in 1.5% uranyl acetate for 2 × 15 s. Samples were examined with Talos 120 C (FEI, Eindhoven, The Netherlands) operating at 120 kV. Micrographs were acquired with a Ceta 16 M CCD camera (FEI, Eindhoven, Netherlands) using TEM Image & Analysis software ver. 4.14 (FEI).

For the TEM investigation, THP-1 cells were fixed with 2.5% glutaraldehyde in 0.1 M sodium cacodylate buffer,

washed and scratched off from the culture plate. Cell suspensions were post fixed in 1% osmium tetroxide, dehydrated with ethanol, propylene oxide and finally embedded in Spurr resin (TAAB, Aldermaston, Berks, England), according to standard procedures.[45] After fixation, the cells were sectioned with an ultramicrotome into 80-nm thick sections. Sections were contrasted with uranyl acetate and lead citrate and examined with a JEM 1230 transmission electron microscope (JEOL, Sollentuna, Sweden) operating at 80 kV. Micrographs were acquired with a Gatan Orius 830 2k × 2k CCD camera (Gatan, Abingdon, Great Britain) using digital micrograph software.

Peri-implantitis biopsy

Two patients participated in the present study, one with a severe peri-implantitis and one with a severe periodontitis. Both patients were scheduled for surgical periodontal treatment at the specialist clinic in periodontology, University Hospital of Umeå, Sweden. Informed written approval was given by both subjects, and authorization for the study was obtained from the Regional Ethical Review Board at Umea University, Sweden (Dnr. 2013–337-31M, 2016–417-32M). Tissue removed during surgery from the peri-implant and periodontal mucosa, respectively, was obtained for examination with transmission electron microscopy. The peri-implantitis patient had a prosthetic supraconstruction made of Ti-porcelain without an abutment and the periodontitis patient periodontal surgery was performed on a tooth reconstructed with amalgam and composite.

Tissues were fixed with 2.5% glutaraldehyde in 0.1 M phosphate buffer, cut into smaller pieces and post fixed in 1% osmium tetroxide, dehydrated with ethanol, a final step in propylene oxide and embedded in resin according to standard procedures. Sections were contrasted with uranyl acetate, Reynold's lead citrate and examined with a Talos 120 C (FEI) operating at 120 kV. Micrographs were acquired with a Ceta 16 M CCD camera (FEI) using TEM Image & Analysis software ver. 4.14 (FEI)

Image analysis of protein aggregates

TEM images of formed protein aggregates were analysed with Fiji (http://fiji.sc/),[46] a scientific image processing application based on ImageJ (https://imagej.nih.gov/ij/).[47] Total area of the TEM images was 17.10 × 17.10 μm. The size of the formed protein aggregates in the test solutions (Ti 100 μM in RPMI 1640 ± 10% FBS and Ti + Co, 100 μM + 100 μM, in RPMI 1640 + 10% FBS) was quantified with the analyze particles application in Fiji, with a size filter of 2–20,000 nm^2 acquired from two micrographs. A 36-square grid, with a size of 6.25 μm^2, was applied on each image ($n = 2$), and the number of protein aggregates in each grid was quantified in the test solutions.

Statistical analysis

Prims v7.0c (GraphPad Software, La Jolla) was used for the statistical analyses. Data from the released IL-1β and viability of THP-1 cells exposed to Ti-Co or Ti-Cr were normalized against the release from Ti 100 μM, which was set as 100%. For parametric tests, one-way ANOVA was used for the variance analysis (IL-1β release, viability and number of particles/grid) with a Tukey test for multiple comparisons between each pair of tested groups; for the nonparametric tests, Kruskal–Wallis H test for the variance analysis of Ti concentration in; cell medium; after filtration and centrifugation; and in cells and supernatant with a Dunn's test for multiple comparisons between tested groups was performed. Un-paired t test with a Welch correction, was used for variance analysis of size of aggregates formed in the tested groups, which were examined with TEM. Mean ± SD of IL-1β release was calculated from experiments repeated three times with four to eight replicates in each experiment.

Statistical significance level was set to $p < 0.05$ in all analyses.

RESULTS

Pro-inflammatory activation and viability of human macrophages after exposure to challenge agents

The cells that were simultaneously exposed to 100 μM Ti + 100 μM Co released much less IL-1β than those exposed to Ti alone, 32.0% ± SD 22.8% vs. 100% ± 15.1%, respectively [Fig. 1(A), $p < 0.001$]. When compared with the negative controls, 21.0% ± 11.6%, no differences were found, showing that Co completely inhibited the pro-inflammatory effect of Ti ($p = 0.1$). Cells exposed to 100 μM Ti and Co, in the concentration range 12.5–50 μM, did not reduce the IL-1β significantly compared with the positive control [Fig. 1(A), $p = 0.2$]. Viability of the cells was not affected by exposure to Ti and Co in the tested concentration range. Therefore, the null hypothesis could be rejected.

Ti in combination with Cr in the tested concentration range 12.5–100 μM did not have the same inhibitory effect on IL-1β release as Co, 77.5% ± 40.6% (Ti + 100 μM Cr) [Fig. 1(B)]. Cr showed a slight increased release of IL-1β at 25 μM compared with the positive control ($p = 0.01$), 131.0% ± 41.2%. Viability of the cells was not affected in the tested concentration. Cr was therefore not further investigated in the rest of the study.

ICP-AES analysis of Ti (μg/g) content

Ti alone at 100 μM in PBS, RPMI 1640 ± 10% FBS or with Co at 100 μM in RPMI 1640 + 10% FBS, were analysed with ICP-AES to see that all Ti added could be analysed with the method, independent of the medium in which it was dissolved. Mean concentration (μg/g) ± SD found in the tested solution showed: Ti-PBS, 5.22 ± 0.06; Ti-RPMI 1640, 5.70 ± 0.07; Ti-RPMI 1640 + 10% FBS, 5.50 ± 0.06; and Ti-Co-RPMI 1640 + 10% FBS, 5.53 ± 0.72. No differences were found between the tested solutions ($p = 0.5$), so different media did not influence the quantification by the ICP-AES instrument [Fig. 2(A)].

After centrifugation at 12,000g for 10 min, the pellet and supernatant of the tested solutions were analysed with ICP-AES. In the solution with Ti in RPMI 1640 + 10% FBS, most of the Ti was found in the analysed pellet and less in the supernatant, mean concentration (μg/g) ± SD, 3.77 ± 0.25 and 0.92 ± 0.32, respectively [Fig. 2(B)]. In the test solutions

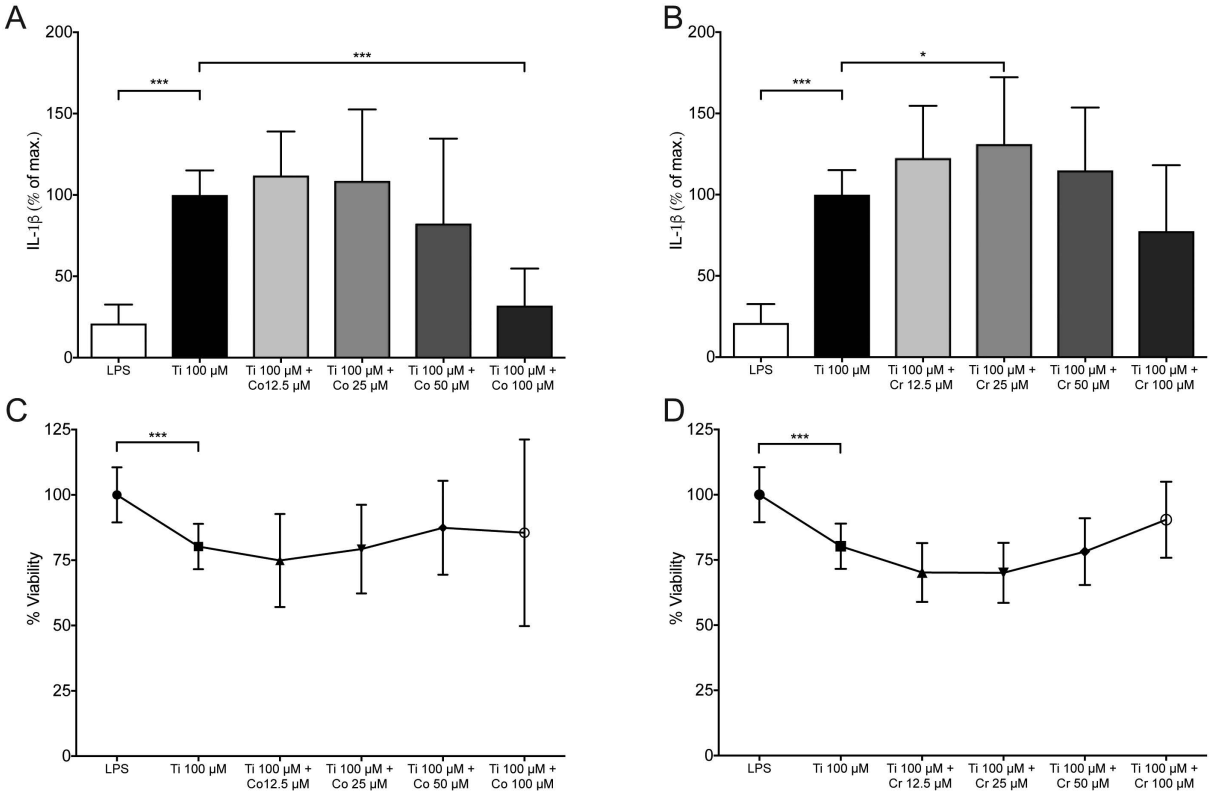

FIGURE 1. IL- 1β release and viability of human macrophages. Mean ± *SD*. *$p < 0.05$, **$p < 0.01$, ***$p < 0.001$. (A) IL-1β release from cells exposed to Ti alone (100 μM) ($n = 12$) or with Co (12.5–100 μM) ($n = 12$/concentration). Cells only primed with *E. coli* lipopolysaccharides (LPS) are used as negative control ($n = 12$). Mean of three repeated experiments. (B) IL-1β release from cells exposed to Ti alone (100 μM) ($n = 12$) or with Cr (12.5–100 μM) ($n = 12$/concentration). Negative control ($n = 12$). Mean of three repeated experiments. (C) Viability (% NRU) of cells exposed to Ti alone (100 μM) ($n = 12$) or with Co (12.5–100 μM) ($n = 5$/concentration). NRU = neutral red uptake. (D) Viability (% NRU) of cells exposed to Ti alone (100 μM) ($n = 12$) or with Cr (12.5–100 μM) ($n = 5$/concentration).

where Co had been present the opposite pattern was found: less of the Ti was found in the pellet and more was found in the supernatant. Mean concentration (μg/g) ± *SD* for pellet and supernatant, 2.09 ± 0.05 and 4.04 ± 0.11, respectively.

No pellet was obtained by centrifugation of Ti in RPMI 1640. When analysed with ICP-AES, all the Ti was found in the supernatant, 5.49 ± 0.13. The concentration of Ti in the pellet after centrifugation of Ti-RPMI 1640 + 10% FBS was higher than in the pellets from the other two tested solutions ($p < 0.001$).

The filtered solutions of 100 μM Ti-RPMI 1640 + 10% FBS showed less Ti than the unfiltered solutions, mean (μg) ± *SD*, 3.24 ± 0.31 vs. 5.00 ± 0.10, respectively. The filtered solutions with 100 μM added Co showed less Ti than the unfiltered solutions, mean (μg) ± *SD*, 2.52 ± 0.16 vs. 5.53 ± 0.71, respectively. When the filtered solutions from the tested groups were compared, the Ti level was lower in the Ti-Co group ($p = 0.04$) [Fig. 2(C)].

ICP-AES analysis of lysed THP-1 cells exposed to Ti 100 μM RPMI 1640 + 10% FBS and supernatants showed that most of the Ti was found in the supernatant, 3.39 ± 0.76 and not in the cells 1.11 ± 0.76 ($p < 0.001$) [Fig. 2(D)]. In the other test group exposed to Ti-Co 100 μM RPMI 1640 + 10% FBS, the highest concentration of Ti was also found in the supernatant, 2.98 ± 1.04 and not in the lysed cells 1.65 ± 1.29 ($p < 0.01$). No differences were found in concentration of Ti in the cells between the groups ($p = 0.2$).

Transmission electron microscopy image (TEM) and image analysis of formed aggregates

After 24 h of incubation of 200 μM Ti in RPMI 1640 + 10% FBS, aggregates with a high electron density were formed and could be investigated in the transmission electron microscope [Fig. 3(A–C)]. Formed complexes have the appearance of a protein aggregate with nanofilament-like structures around the edges. In the test group with Ti and Co, a different appearance in size and structure of the aggregates are shown [Fig. 3(D–F)]. Aggregates in the Ti-Co group are coated with exosome like structures, which cannot be seen in Ti group. Exosome structures seen in the images are not coated with metal, indicated by the low electron density. When comparing images of the Ti group containing FBS with the Ti-Co group, a larger number and smaller size of assembled aggregates can be seen in the Ti group, which also could be confirmed with the image analysis with Fiji. Image analysis of two randomly selected images from each group confirmed that the Ti group contained more aggregates than the Ti-Co group, $n = 2{,}348$ and $n = 1{,}071$, respectively. Two of the images used for the

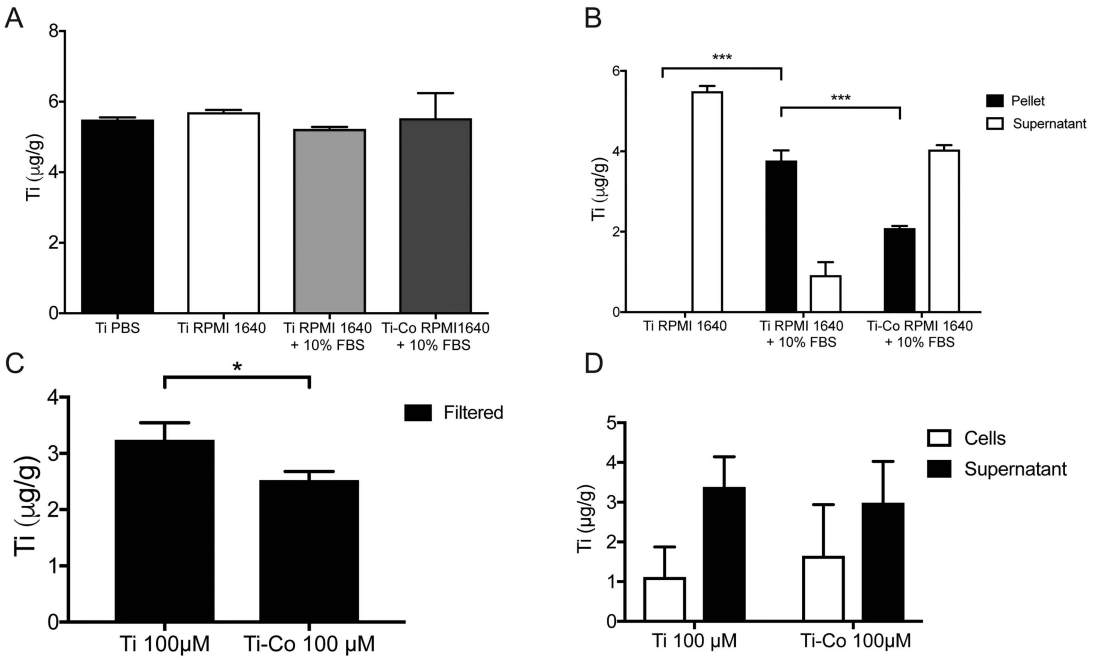

FIGURE 2. ICP-AES analysis of Ti (µg/g) content. Mean $*p < 0.05$, $***p < 0.001$. (A) Ti content after culture in different media. No differences are found among the tested groups (mean of 3 samples/group) ($p = 0.5$). (B) Ti content in pellet ($n = 3$) and supernatant ($n = 3$) after culture in different media. (C) Ti content in solution after culture without ($n = 3$) or with Co ($n = 3$) and filtration through a 0.22-µm sterile filter. (D) Ti content in lysed cells and supernatant after 24-h exposure to Ti ($n = 12$) or Ti + Co ($n = 12$), both suspended in RPMI 1640 + 10% FBS. No differences in Ti content in cells ($p = 0.5$) or supernatant ($p = 0.7$) are found.

particle analysis are shown in Figure 3A,D. Size distributions show that a majority of the registered aggregates have an area in the interval 2–10 nm^2 for both solutions [Fig. 4(A)].

Aggregate size of the formed aggregates in the Ti-Co group was larger than in the Ti group, mean size (nm^2) ± *SD*, 40.31 ± 285.5 vs. 15.99 ± 33.09, respectively [Fig. 4(B)]. Size analysis was not performed for Ti RPMI 1640, because only single aggregates were found in the images.

When a 36-square grid was placed on the images for all three groups and number of particles was registered, Ti RPMI 1640 + 10% FBS contained more aggregates (25.5 ± 4.56/grid) ($p < 0.001$)), than either Ti RPMI 1640, (0.06 ± 0.23/grid) or Ti-Co RPMI 1640 + 10% FBS, (13.33 ± 4.14/grid) [Fig. 4(C)].

Uptake of Ti protein aggregates in human macrophages in vitro investigated with transmission electron microscopy (TEM)

Aggregates with a high electron density could be identified within the sectioned macrophages. In macrophages exposed to Ti alone aggregates could be seen inside the cytoplasm with a surrounding membrane, with an appearance that resembles a phagolysosome [Fig. 5(A–C)]. No high electron density particles or similar aggregates were found within the macrophages in the control sections that had only been exposed to cell medium (images not shown).

Cells exposed to a combination of Ti and Co showed a different appearance. Aggregates with a high electron density were identified within the cells, but the aggregates were more concentrated and were not surrounded by a cell membrane as in the cells exposed to Ti alone. The identified aggregates are also found more freely in the cell cytoplasm without a visible membrane [Fig. 5(D–F)]. In the control section, this type of electron-dense aggregates, without a surrounding membrane, was not found.

Transmission electron microscopy image (TEM) of peri-implantitis mucosa

Phagocytes could be identified in the peri-implantitis sections [Fig. 6(A)]. Similar structures as found in the *in vitro* experiment with macrophages exposed to Ti, exhibiting aggregates with high electron density and surrounded by a membrane, were identified in the peri-implantitis sections. As in the *in vitro* sections, the structures that contained the aggregates resembled the appearance of a phagolysosome [Fig. 6(B–D)]. No structures with the same appearance were identified in the periodontitis sections (images not shown).

DISCUSSION

Data from the present study show that Ti-ions form aggregates with serum proteins that are phagocytized by macrophages and located in membrane-surrounded lysosome-like compartments. Prolonged incubation caused activation and release of IL-1β from the exposed macrophages. Our method for detection of IL-1β recognizes only the active form of the cytokine, indicating a cleavage of pro-IL-1β that is secreted in its active form. IL-1β play a crucial role in the inflammatory process and by measuring the release of IL-1β it can be used as a marker for assembly of the inflammasome complex in macrophages after exposure to Ti.[31,48]

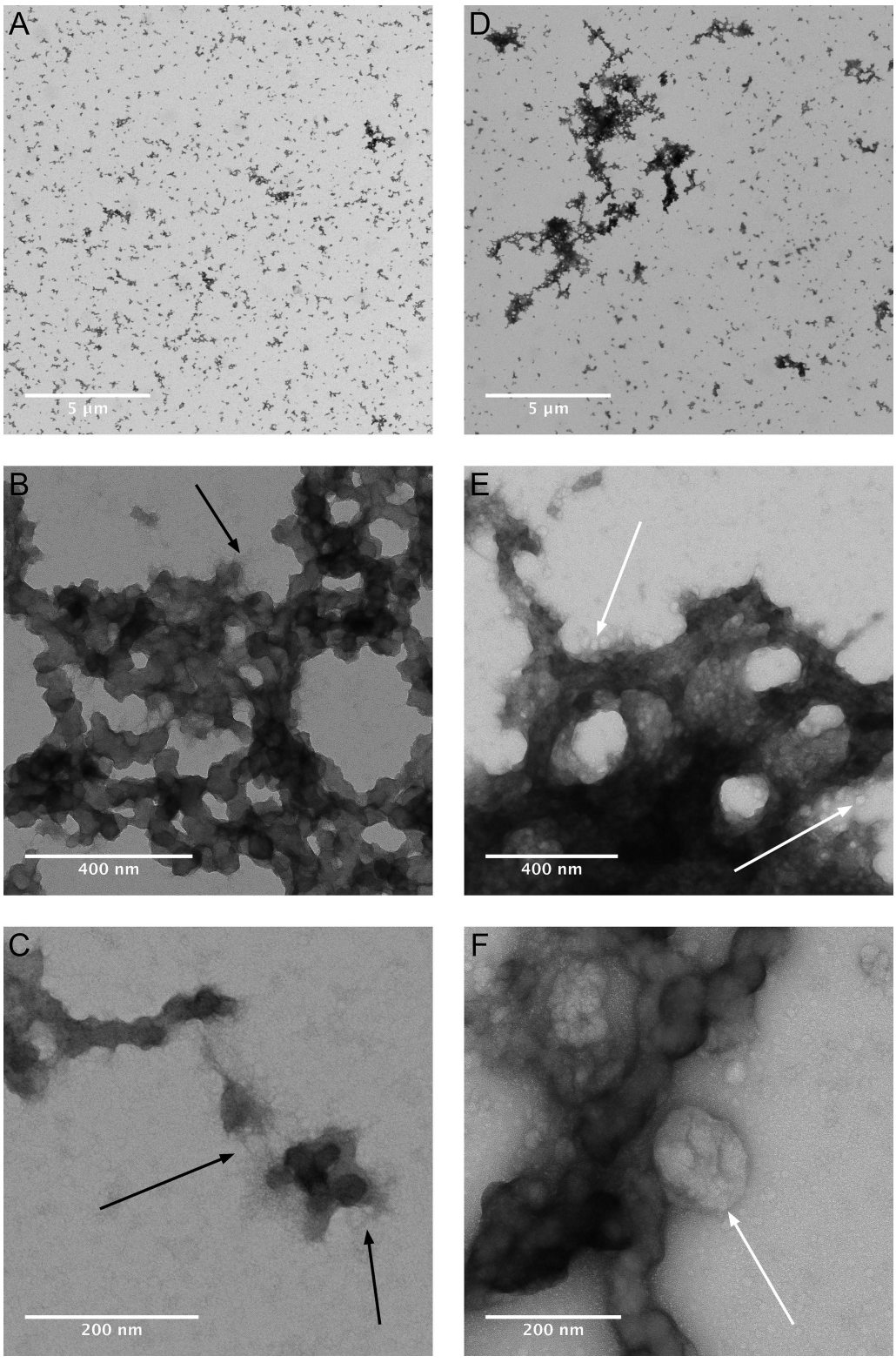

FIGURE 3. Transmission electron micrographs show aggregate morphology after incubation of RPMI 1640 + 10% FBS with Ti (A-C) or Ti + Co (D-F) without the presence of macrophages. Magnification increasing from A to C and from D to F. Nano-filament like structures are seen at the edges of the aggregates (C). Protein aggregates are larger and more electron dense with Ti + Co (D-F) than with only Ti (A–C). Filament (B, C) and exosome (E, F) like structures indicated with black- and white arrows.

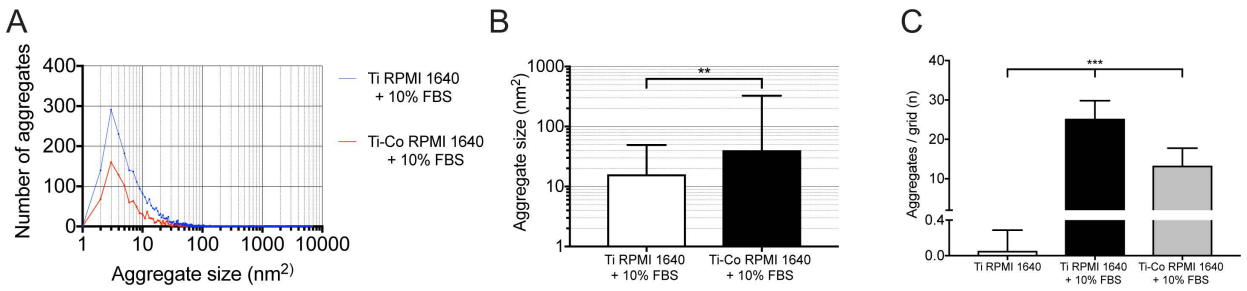

FIGURE 4. Image analysis of aggregates formed by Ti and Ti + Co in RPMI 1640 + FBS without the presence of macrophages. (A) Size distribution of protein aggregates with Ti (blue) or Ti + Co (red). Data are based on aggregates found in two randomly selected images from each group, Ti aggregates ($n = 2348$) and for Co ($n = 1071$). (B) Aggregate size formed with Ti (open bar) or Ti + Co (solid bar). Mean ± *SD*. ** $p < 0.01$ (C) Number of formed aggregates per grid with Ti (black bar) or Ti + Co (grey bar). Essentially no aggregates were formed in the absence of FBS. Mean ± *SD* from two randomly selected images (number of grids/image = 36). *** $p < 0.001$.

Addition of cobalt ions in the solution neutralized the Ti-induced inflammatory effect in the exposed macrophages. Concentrations of Co used in the present study, did not show any evidence for an increased release of IL-1β mediated through the inflammasome complex by Co in our previous study.[31] TEM analyses indicated that the Ti-Co aggregates were freely present in the cytosol and lacked a surrounding intracellular membrane. In addition, the size and the structure of the formed metal-protein aggregates differed in the various solutions, and this might be of importance for the pro-inflammatory response. Cr, on the other hand, did not show the same ability to neutralize the release of active IL-1β as did Co. It is previously known that magnesium can decrease the production of pro-inflammatory cytokines, for example, TNF-α and IL-6,[49] and our findings that Co reduces a Ti-induced pro-inflammatory response are interesting.

Cells exposed to 100 μM Ti during the 24 h prior to priming with *E. coli* LPS showed a pro-inflammatory activation as measured by release of the active form of IL- β in line with results from a previous study.[31]

Co is considered as a toxic agent in most studies but might in sub-toxic concentrations promote angiogenesis as suggested in a review by Vasconcelos et al.[50] In the present study, neither Co nor Cr addition impaired cell viability as compared with Ti alone. This is supported by a previous study where Co not affected the viability of THP-1 cells in concentrations up to 200 μM.[31] As cytotoxicity test, NRU has previously been validated as a good technique for quantification of viable cells.[44] Our results showed that IL-1β released in the protein detection analysis was measured in noncytotoxic conditions.

The interesting finding, that Co is able to block or change the formations of pro-inflammatory aggregates, suggests that further investigations need to examine formation of Ti aggregates and their cellular uptake.

We could confirm that Co changes the size and number of aggregates formed in Ti-protein solutions, as documented by transmission electron microscopy. The microscope used in this study was a conventional TEM, without the possibility to perform element analysis. A scanning transmission electron microscope with the possibility to perform element mapping with energy-dispersive X-ray spectroscopy (EDS) could have added further information about the formed aggregates but was not applicable in this study.

It has previously been shown that particle size is crucial for the induced pro-inflammatory response.[23,24,51] Image analysis showed that serum proteins are needed for aggregate formation, and when Co was added, aggregates were larger, but fewer than those formed by Ti alone. Investigation of aggregate formation in different media, centrifugation and filtering, confirmed that serum proteins are necessary for the formation of the Ti aggregates. Also, larger but fewer aggregates are formed when Co is present in the solution. Filtering reduced the concentration of Ti in the solutions. Since most of the Ti aggregates passed through the filter, then most of the formed aggregates are smaller than 0.22 μm, which was confirmed by the particle analysis of the TEM images. The differences in the appearance (for example, exosome-like structures) and size of protein aggregates formed when Co was present in the solution are interesting. Therefore, how Co affects uptake of protein aggregates by macrophages should be further investigated.

Using TEM, formed Ti aggregates were found within the macrophages, and the aggregates were surrounded by a visible membrane, which showed similarity to lysosomes. These high electron-dense aggregates, surrounded by a membrane, were not found in the control solution without any Ti in the test solution. When cells were exposed to Ti and Co in combination, another pattern occurred. Clusters of highly electron-dense aggregates were concentrated in the cytoplasm without a limiting membrane. This finding suggests that the pathways for cell uptake differ when Co is present. Attempts to apply element mapping with SEM-EDS was performed, but the Ti content in the sections was below the detection level, which resulted in destruction of the samples by the electron beam.

Surprisingly, we found no differences in the Ti uptake of the cells exposed to Ti with or without addition of Co in the ICP-AES analysis. This finding indicates that the effect of Co is mediated through inhibition of phagolysosomal translocation of metal aggregates rather than affecting the cellular uptake of the metal-protein aggregates. It has previously been shown that uptake of nondegradable material into the phagolysosomes induces activation of the inflammasome in macrophages and consequently activation and release of IL-

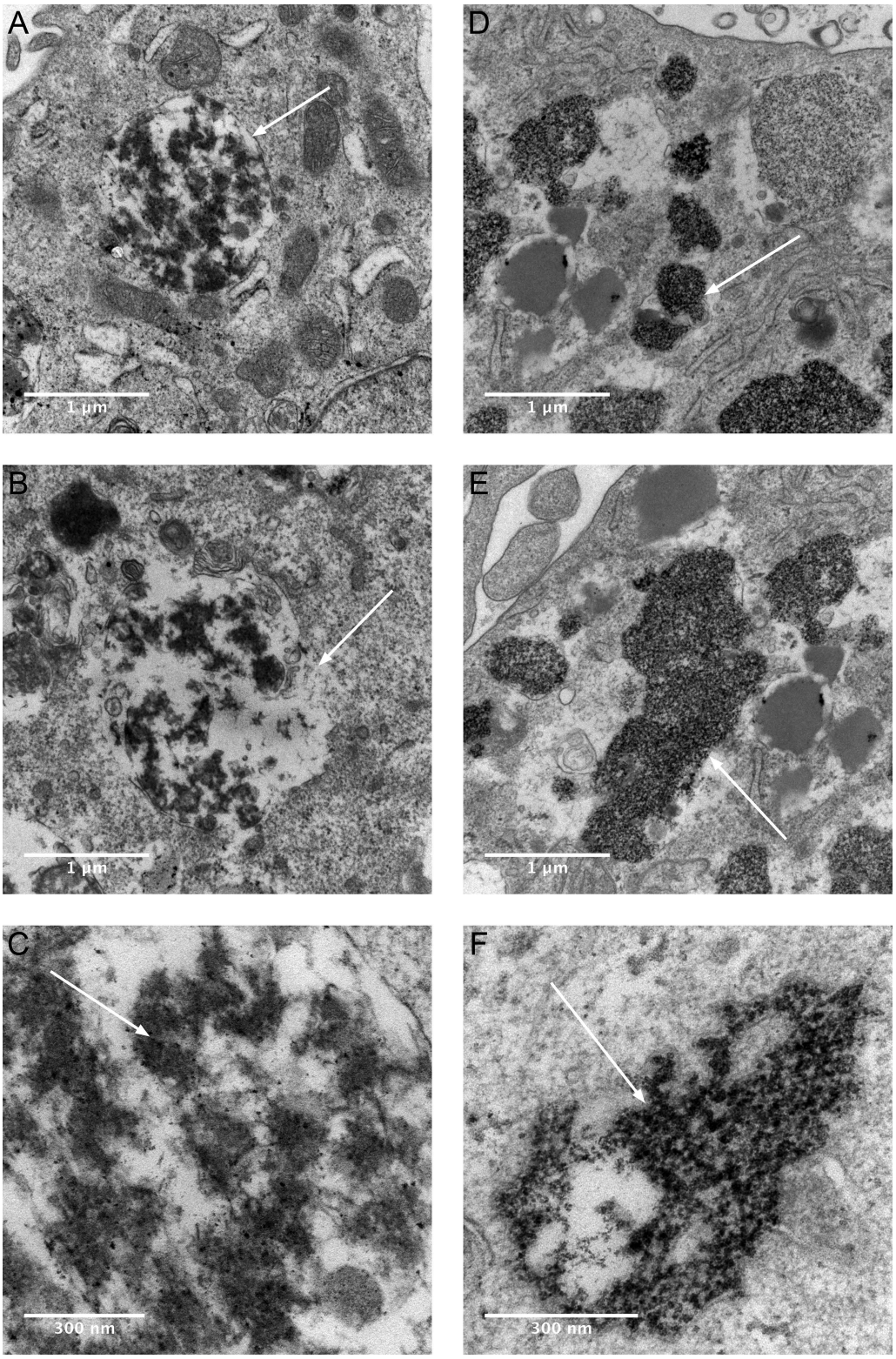

FIGURE 5. Electron micrographs show aggregate uptake into human macrophage THP-1 cells *in vitro* after exposure to Ti (A-C) or Ti + Co (D-F) with RPMI 1640 + 10% FBS medium. Transmission electron micrograph images are shown in two different magnifications. Uptake of Ti-protein aggregates with a surrounding membrane (A, white arrow), and that structure shows some similarity to a phagolysosome. Destruction of the lysosomal membrane, which contains high-density Ti aggregates (B, white arrow). Visible Ti nanoparticles inside lysosome (C, white arrow). Ti-Co protein aggregates are more concentrated, located freely in the cytoplasm, and have no visible surrounding membrane (D–F) compared with Ti aggregates (A–C). High density cluster of metal aggregates inside the cytoplasm (D, white arrow). No visible membrane surrounding the metal-rich cluster of protein aggregates (E, F, white arrow).

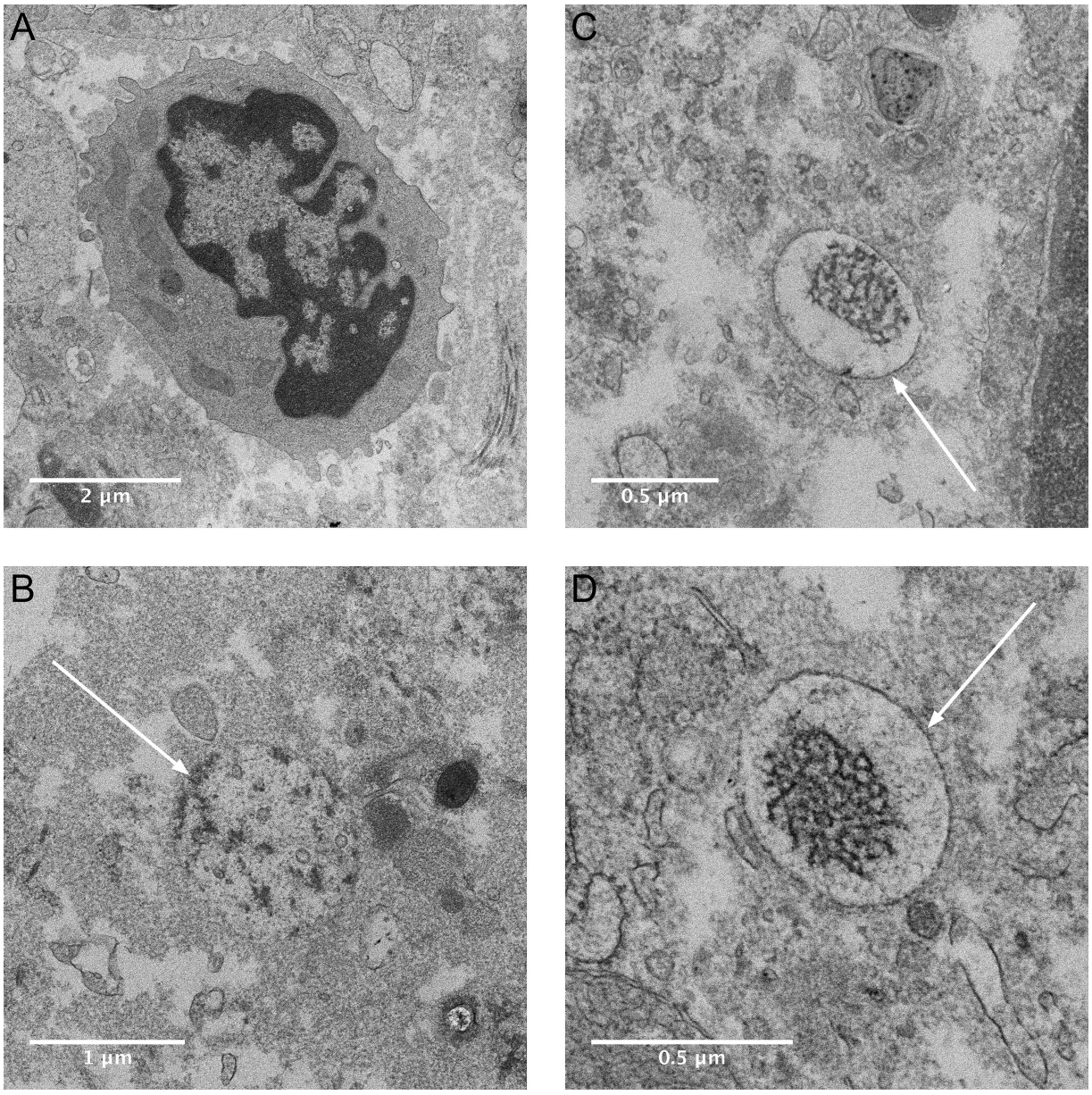

FIGURE 6. Electron micrographs showing phagocyte and intracellular aggregates in human peri-implantitis biopsy. Host cell with macrophage like structures (A). Intracellular structures with electron-dense content with various membrane structure (indicated with arrows) (B–D) similar to that found in the THP-1 cells exposed to Ti RPMI 1640 + 10% FBS. No similar structures were found in the sections of tissue from the periodontitis biopsy (not shown).

1β.[40] Initiation of pro-IL-1β expression in macrophages is triggered through the toll-like receptor (TLR)-4, and Ti can work as a secondary stimulus by activation of the multiprotein inflammasome.[31,40]

Particulate debris of Ti is known to induce an increased level of the pro-inflammatory cytokines IL-1β, IL-6, and TNF-α in cultured macrophages.[52–54] We previously showed that human macrophages exposed to Ti solutions activate and release IL-1β,[31] possibly by phagocytosis of formed Ti aggregates in physiological solution. Phagocytosis of wear and soluble particles by macrophages is suggested as the pathway for induction and release of pro-inflammatory cytokines for example, IL-1β.[23,55,56]

In addition, it has been shown that polarization of macrophages to M1 (pro-inflammatory) and M2 (anti-inflammatory) macrophages is important in the inflammatory response in the tissue.[57] A recent article by Kumanto et al. showed that Co shifted the polarization of resting macrophages to an M2 phenotype, and that the balance of inducible nitric oxidase synthase (iNos), NADPH oxidase (NOX) 2 and IL-6 could be changed in LPS-activated macrophages.[42] These findings might explain our discovery that Co inhibited the Ti-induced IL-1β release from LPS-stimulated macrophages, and therefore represents an interesting target for further investigations.

Similar aggregates as seen *in vitro* of macrophages exposed to Ti, with a visible membrane structure, were

found in the human peri-implantitis biopsy tissue. In the human periodontitis biopsy tissue, no similar highly electron-dense aggregates with a surrounding membrane were found. This indicates that Ti aggregates are present in the peri-implantitis tissue, they are phagocytized by macrophages, and this might escalate the inflammatory reaction in the tissue. However, the effect of Ti-particles is negligible without an initial priming of the macrophages with stimuli of microbial origin.[31] Unfortunately, element composition analysis with SEM-EDS could not be performed due to that the concentration in the lysosomal structure was under the detection level of the instrument.

By combining biochemical and imaging analyzes the obtained quantitative data could be better explained. The choice of ICP-MS as the method for analysis is most often done if the expected concentration in the measuring solution of Ti or Co is below 5 ng/mL.[58,59] When higher concentrations are expected, the ICP-AES will be preferred because it gives better accuracy and less interferences.[59] The concentrations used of the analytes Ti and Co in this study were mostly between 50 and 5000 ng/mL, so the ICP-AES is hence a better choice.[58,60] Moreover, all of the methodology of the analysis has previously been used and validated by other researchers.

The TEM images of the formed Ti aggregates in the present study were very similar to the solubilized TiO_2 nanoparticles in human serum, which were shown by Soto-Alvaredo et al.[61] Uptake of phagocytized TiO_2 in endothelial cells[62] and osteoblasts[63] appear similar to our present findings *in vitro* and in human peri-implantitis tissue. We have shown in this study that phagocytized Ti aggregates could be found in human macrophages *in vitro* as well in peri-implantitis tissue. It cannot be ruled out that the Ti from the dental implant might contribute to the inflammatory response in peri-implant tissue and might lead to a peri-implantitis.

From the results of the present study, it can be speculated that a supra-construction in a Co-Cr alloy on the dental implant, might inhibit the inflammatory response from macrophages in the peri-implant tissue induced by Ti. This pro-inflammatory effect of Ti is probably negligible in a healthy periodontium but could be tremendous in combination with microorganisms that act in synergy to activate macrophages.

Positive treatment outcomes have been shown in the short term for peri-implantitis, but diversity in the reports and that long-term success of therapy is unknown. This makes it not possible to give evidence-based recommendation for therapy at this time.[64,65] Therefore, it is crucial to find the causes of peri-implantitis and try to minimize them, so that unnecessary patient suffering and costs can be avoided.

CONCLUSION

In the present study, we show that Co can neutralize the Ti-induced activation and release of IL-1β in human macrophages *in vitro*. Serum proteins are needed for the formation of metal-protein aggregates in cell medium and the structures of the aggregates as well as the localisation after cellular uptake differ if Co is present in a Ti solution. Phagocytized aggregates with a similar appearance seen *in vitro* with Ti present, were also visible in a sample from human peri-implant tissue.

ACKNOWLEDGEMENTS

Granted by Västerbotten county funding (TUA, VLL 1147–2014) and Swedish Dental Society. Thanks to the Department of Periodontology at Umeå University Hospital, Sweden, for the help with biopsies. Also, a special thanks to Sara Henriksson at Umeå Core Facility for Electron Microscopy (UCEM), Umeå University, Sweden, for the help with the transmissions electron microscopy.

CONFLICT OF INTERESTS

No benefit of any kind will be received either directly or indirectly by the authors.

REFERENCES

1. Branemark PI, Adell R, Breine U, Hansson BO, Lindstrom J, Ohlsson A. Intra-osseous anchorage of dental prostheses. I. Experimental studies. Scand J Plast Reconstr Surg 1969;3:81–100.
2. Brunette DM. Titanium in Medicine: Material Science, Surface Science, Engineering, Biological Responses and Medical Applications. Berlin: Springer; 2001.
3. Steinemann SG. Titanium–the material of choice?. Periodontol 2000 1998;17:7–21.
4. Roach M. Base metal alloys used for dental restorations and implants. Dent Clin North Am 2007;51:603–627.
5. Zitzmann NU, Berglundh T. Definition and prevalence of peri-implant diseases. J Clin Periodontol 2008;35:286–291.
6. Koldsland OC, Scheie AA, Aass AM. Prevalence of peri-implantitis related to severity of the disease with different degrees of bone loss. J Periodontol 2010;81:231–238.
7. Derks J, Tomasi C. Peri-implant health and disease. A systematic review of current epidemiology. J Clin Periodontol 2015;42: S158–S171.
8. Schuldt Filho G, Dalago HR, Oliveira de Souza JG, Stanley K, Jovanovic S, Bianchini MA. Prevalence of peri-implantitis in patients with implant-supported fixed prostheses. Quintessence Int 2014;45:861–868.
9. Daubert DM, Weinstein BF, Bordin S, Leroux BG, Flemmig TF. Prevalence and predictive factors for peri-implant disease and implant failure: A cross-sectional analysis. J Periodontol 2015;86: 337–347.
10. Gurgel BCV, Montenegro SCL, Dantas PMC, Pascoal ALB, Lima KC, Calderon PDS. Frequency of peri-implant diseases and associated factors. Clin Oral Implants Res 2017;28:1211–1217.
11. Rokn A, Aslroosta H, Akbari S, Najafi H, Zayeri F, Hashemi K. Prevalence of peri-implantitis in patients not participating in well-designed supportive periodontal treatments: A cross-sectional study. Clin Oral Implants Res 2017;28:314–319.
12. Schwarz F, Becker K, Sahm N, Horstkemper T, Rousi K, Becker J. The prevalence of peri-implant diseases for two-piece implants with an internal tube-in-tube connection: A cross-sectional analysis of 512 implants. Clin Oral Implants Res 2017;28:24–28.
13. Jepsen S, Berglundh T, Genco R, Aass AM, Demirel K, Derks J, Figuero E, Giovannoli JL, Goldstein M, Lambert F, Ortiz-Vigon A, Polyzois I, Salvi GE, Schwarz F, Serino G, Tomasi C, Zitzmann NU. Primary prevention of peri-implantitis: Managing peri-implant mucositis. J Clin Periodontol 2015;42: S152–S157.
14. Mombelli A, Lang NP. The diagnosis and treatment of peri-implantitis. Periodontol 2000 1998;17:63–76.
15. Safioti LM, Kotsakis GA, Pozhitkov AE, Chung WO, Daubert DM. Increased levels of dissolved titanium are associated with peri-implantitis - A cross-sectional study. J Periodontol 2017;88:436–442.
16. Albrektsson T, Canullo L, Cochran D, De Bruyn H. Peri-implantitis": A complication of a foreign body or a man-made

"disease". Facts and fiction. Clin Implant Dent Relat Res 2016;18: 840–849.
17. Lindhe J, Meyle J. Group DoEWoP. Peri-implant diseases: Consensus Report of the Sixth European Workshop on Periodontology. J Clin Periodontol 2008;35:282–285.
18. Lang NP, Berglundh T. Working Group 4 of Seventh European Workshop on P. Periimplant diseases: Where are we now?–Consensus of the Seventh European Workshop on Periodontology. J Clin Periodontol 2011;38:178–181.
19. Mombelli A, Muller N, Cionca N. The epidemiology of peri-implantitis. Clin Oral Implants Res 2012;23:67–76.
20. Albrektsson T, Dahlin C, Jemt T, Sennerby L, Turri A, Wennerberg A. Is marginal bone loss around oral implants the result of a provoked foreign body reaction?. Clin Implant Dent Relat Res 2014;16:155–165.
21. Harris WH, Schiller AL, Scholler JM, Freiberg RA, Scott R. Extensive localized bone resorption in the femur following total hip replacement. J Bone Joint Surg Am 1976;58:612–618.
22. Purdue PE, Koulouvaris P, Potter HG, Nestor BJ, Sculco TP. The cellular and molecular biology of periprosthetic osteolysis. Clin Orthop Relat Res 2007;454:251–261.
23. Caicedo MS, Desai R, McAllister K, Reddy A, Jacobs JJ, Hallab NJ. Soluble and particulate Co-Cr-Mo alloy implant metals activate the inflammasome danger signaling pathway in human macrophages: A novel mechanism for implant debris reactivity. J Orthop Res 2009;27:847–854.
24. Hallab NJ, Jacobs JJ. Biologic effects of implant debris. Bull NYU Hosp Jt Dis 2009;67:182–188.
25. Burton L, Paget D, Binder NB, Bohnert K, Nestor BJ, Sculco TP, Santambrogio L, Ross FP, Goldring SR, Purdue PE. Orthopedic wear debris mediated inflammatory osteolysis is mediated in part by NALP3 inflammasome activation. J Orthop Res 2013;31:73–80.
26. Gallo J, Vaculova J, Goodman SB, Konttinen YT, Thyssen JP. Contributions of human tissue analysis to understanding the mechanisms of loosening and osteolysis in total hip replacement. Acta Biomater 2014;10:2354–2366.
27. Samelko L, Landgraeber S, McAllister K, Jacobs J, Hallab NJ. Cobalt alloy implant debris induces inflammation and bone loss primarily through danger signaling, not TLR4 activation: Implications for DAMP-ening Implant Related Inflammation. PLoS One 2016;11:e0160141.
28. Hallab NJ, Jacobs JJ. Chemokines associated with pathologic responses to orthopedic implant debris. Front Endocrinol (Lausanne) 2017;8:5.
29. Ingham E, Fisher J. The role of macrophages in osteolysis of total joint replacement. Biomaterials 2005;26:1271–1286.
30. Berglundh T, Zitzmann NU, Donati M. Are peri-implantitis lesions different from periodontitis lesions?. J Clin Periodontol 2011; 38(Suppl 11): 188–202.
31. Pettersson M, Kelk P, Belibasakis GN, Bylund D, Molin Thoren M, Johansson A. Titanium ions form particles that activate and execute interleukin-1beta release from lipopolysaccharide-primed macrophages. J Periodontal Res 2017;52:21–32.
32. Dinarello CA. Biologic basis for interleukin-1 in disease. Blood 1996;87:2095–2147.
33. O'Neill LAJ, Dinarello CA. The IL-1 receptor/toll-like receptor superfamily: Crucial receptors for inflammation and host defense. Immunol Today 2000;21:206–209.
34. Davis BK, Wen HT, Ting JPY. The Inflammasome NLRs in Immunity, Inflammation, and Associated Diseases. In: Paul WE, Littman DR, Yokoyama WM, editors. Annu Rev Immunol 2011;29:707–735.
35. Irshad M, Scheres N, Crielaard W, Loos BG, Wismeijer D, Laine ML. Influence of titanium on in vitro fibroblast-Porphyromonas gingivalis interaction in peri-implantitis. J Clin Periodontol 2013; 40:841–849.
36. Makihira S, Mine Y, Nikawa H, Shuto T, Iwata S, Hosokawa R, Kamoi K, Okazaki S, Yamaguchi Y. Titanium ion induces necrosis and sensitivity to lipopolysaccharide in gingival epithelial-like cells. Toxicol in Vitro 2010;24:1905–1910.
37. Wachi T, Shuto T, Shinohara Y, Matono Y, Makihira S. Release of titanium ions from an implant surface and their effect on cytokine production related to alveolar bone resorption. Toxicology 2015; 327:1–9.
38. Sund J, Palomaki J, Ahonen N, Savolainen K, Alenius H, Puustinen A. Phagocytosis of nano-sized titanium dioxide triggers changes in protein acetylation. J Proteomics 2014;108:469–483.
39. Eger M, Sterer N, Liron T, Kohavi D, Gabet Y. Scaling of titanium implants entrains inflammation-induced osteolysis. Sci Rep 2017; 7:39612.
40. Guo H, Callaway JB, Ting JP. Inflammasomes: Mechanism of action, role in disease, and therapeutics. Nat Med 2015;21:677–687.
41. Makihira S, Mine Y, Kosaka E, Nikawa H. Titanium surface roughness accelerates RANKL-dependent differentiation in the osteoclast precursor cell line, RAW264.7. Dent Mater J 2007;26:739–745.
42. Kumanto M, Paukkeri EL, Nieminen R, Moilanen E. Cobalt(II) chloride modifies the phenotype of macrophage activation. Basic Clin Pharmacol Toxicol 2017;121:98–105.
43. Moore GE, Gerner RE, Franklin HA. Culture of normal human leukocytes. JAMA 1967;199:519–524.
44. Repetto G, del Peso A, Zurita JL. Neutral red uptake assay for the estimation of cell viability/cytotoxicity. Nat Protoc 2008;3:1125–1131.
45. Spurr AR. A low-viscosity epoxy resin embedding medium for electron microscopy. J Ultrastruct Res 1969;26:31–43.
46. Schindelin J, Arganda-Carreras I, Frise E, Kaynig V, Longair M, Pietzsch T, Preibisch S, Rueden C, Saalfeld S, Schmid B, Tinevez J-Y, White DJ, Hartenstein V, Eliceiri K, Tomancak P, Cardona A. Fiji: An open-source platform for biological-image analysis. Nat Methods 2012;9:676–682.
47. Schneider CA, Rasband WS, Eliceiri KW. NIH Image to ImageJ: 25 years of image analysis. Nat Methods 2012;9:671–675.
48. Dinarello CA. Interleukin-1 in the pathogenesis and treatment of inflammatory diseases. Blood 2011;117:3720–3732.
49. Sugimoto J, Romani AM, Valentin-Torres AM, Luciano AA, Ramirez Kitchen CM, Funderburg N, Mesiano S, Bernstein HB. Magnesium decreases inflammatory cytokine production: A novel innate immunomodulatory mechanism. J Immunol 2012;188: 6338–6346.
50. Vasconcelos DM, Santos SG, Lamghari M, Barbosa MA. The two faces of metal ions: From implants rejection to tissue repair/ regeneration. Biomaterials 2016;84:262–275.
51. St Pierre CA, Chan M, Iwakura Y, Ayers DC, Kurt-Jones EA, Finberg RW. Periprosthetic osteolysis: Characterizing the innate immune response to titanium wear-particles. J Orthop Res 2010; 28:1418–1424.
52. Blaine T, Rosier R, Puzas J, Looney R, Reynolds P, Reynolds S, O'keefe R. Increased levels of tumor necrosis factor-alpha and interleukin-6 protein and messenger RNA in human peripheral blood monocytes due to titanium particles. J Bone Joint Surg-Am Vol 1996;78:1181–1192.
53. Maloney WJ, James RE, Smith RL. Human macrophage response to retrieved titanium alloy particles in vitro. Clin Orthop Relat Res 1996;268–278.
54. Nakashima Y, Sun DH, Trindade MC, Maloney WJ, Goodman SB, Schurman DJ, Smith RL. Signaling pathways for tumor necrosis factor-alpha and interleukin-6 expression in human macrophages exposed to titanium-alloy particulate debris in vitro. J Bone Joint Surg Am 1999;81:603–615.
55. Pajarinen J, Kouri VP, Jamsen E, Li TF, Mandelin J, Konttinen YT. The response of macrophages to titanium particles is determined by macrophage polarization. Acta Biomater 2013;9:9229–9240.
56. Caicedo MS, Pennekamp PH, McAllister K, Jacobs JJ, Hallab NJ. Soluble ions more than particulate cobalt-alloy implant debris induce monocyte costimulatory molecule expression and release of proinflammatory cytokines critical to metal-induced lymphocyte reactivity. J Biomed Mater Res A 2010;93:1312–1321.
57. Murray PJ. Macrophage polarization. Annu Rev Physiol 2017;79: 541–566.
58. van de WHJ. Determination of elements by ICP-AES and ICP-MS. National Institute of Public Health and the Environment (RIVM). Bilthoven, The Netherlands 2003;19.
59. Bolann BJ, Rahil-Khazen R, Henriksen H, Isrenn R, Ulvik RJ. Evaluation of methods for trace-element determination with emphasis on their usability in the clinical routine laboratory. Scand J Clin Lab Invest 2007;67:353–366.
60. Kunze J, Wimmer MA, Koelling S, Schneider E. Determination of titanium and zirconium wear debris in blood serum by means of

HNO3/HF pressurized digestion using ICP optical emission spectrometry. Fresenius J Anal Chem 1998;361:496–499.
61. Soto-Alvaredo J, Blanco E, Bettmer J, Hevia D, Sainz RM, López Cháves C, Sánchez C, Llopis J, Sanz-Medel A, Montes-Bayón M. Evaluation of the biological effect of Ti generated debris from metal implants: Ions and nanoparticles. Metallomics 2014;6:1702–1708.
62. Halamoda Kenzaoui B, Chapuis Bernasconi C, Guney-Ayra S, Juillerat-Jeanneret L. Induction of oxidative stress, lysosome activation and autophagy by nanoparticles in human brain-derived endothelial cells. Biochem J 2012;441:813–821.
63. Niska K, Pyszka K, Tukaj C, Wozniak M, Radomski MW, Inkielewicz-Stepniak I. Titanium dioxide nanoparticles enhance production of superoxide anion and alter the antioxidant system in human osteoblast cells. Int J Nanomedicine 2015;10:1095–1107.
64. Heitz-Mayfield LJ, Mombelli A. The therapy of peri-implantitis: A systematic review. Int J Oral Maxillofac Implants 2014;29: 325–345.
65. Esposito M, Grusovin MG, Worthington Helen V. Interventions for replacing missing teeth: Treatment of peri-implantitis. Cochrane Database of Systematic Reviews. 2012;1:CD004970.